



**HAL**  
open science

## Experimental characterization of PCI impact on vibrating fuel rod under axial turbulent flow representative of JHR irradiation device ADELINÉ

Veronica d' Ambrosi, Christophe Destouches, Guillaume Ricciardi, Stéphane Breaud, Frédéric Lebon, Jean-Marie Gatt, Jérôme Julien, Daniel Parrat

### ► To cite this version:

Veronica d' Ambrosi, Christophe Destouches, Guillaume Ricciardi, Stéphane Breaud, Frédéric Lebon, et al.. Experimental characterization of PCI impact on vibrating fuel rod under axial turbulent flow representative of JHR irradiation device ADELINÉ. EPJ Web of Conferences, 2020, 225, pp.04007. 10.1051/epjconf/202022504007 . cea-02559143

**HAL Id: cea-02559143**

**<https://cea.hal.science/cea-02559143v1>**

Submitted on 30 Apr 2020

**HAL** is a multi-disciplinary open access archive for the deposit and dissemination of scientific research documents, whether they are published or not. The documents may come from teaching and research institutions in France or abroad, or from public or private research centers.

L'archive ouverte pluridisciplinaire **HAL**, est destinée au dépôt et à la diffusion de documents scientifiques de niveau recherche, publiés ou non, émanant des établissements d'enseignement et de recherche français ou étrangers, des laboratoires publics ou privés.

# Experimental characterization of PCMI impact on vibrating fuel rod representative of JHR irradiation device ADELINÉ

V. D’Ambrosi, C. Destouches, G. Ricciardi, S. Breaud, F. Lebon, JM. Gatt, J. Julien and D. Parrat

**Abstract**—Pellet Clad Mechanical Interaction (PCMI) has been recognized as one of the major concerns to guarantee clad integrity while attempting at increasing the flexibility of PWR nuclear reactor operations to follow grid demand. This has motivated through the years the realization of power ramp tests in dedicated irradiation devices in “Material Testing Reactors” MTR as OSIRIS and SILOE. ADELINÉ, an irradiation device in the next future “Jules Horowitz Reactor” (JHR), is being designed for in-pile experiments of this kind. To improve present knowledge and increase the validation capability of simulation codes, a complex multi-physics measurement method is needed, to characterize all relevant physical quantities involved and impacted by PCMI. Researches are also being carried out to identify innovative methodologies. In this frame, we investigate the technological feasibility of measuring the effects of PCMI on the vibrations of the nuclear fuel rod externally excited by a turbulent axial flowrate. Analytical and numerical models cannot predictively describe the system due to the complexity of non linear interactions occurring in the fuel rod: pellet-pellet friction and pellet-clad shock. The IMPIGRITIA experimental set-up has been thus developed to reproduce the mechanical interaction between pellets and clad in a controlled environment: low pressure, room temperature and out of neutron flux. The designed test bench presents a clamped free single short rod, centered in the test section by means of four centering elements. Different rod configurations are implemented and localized closure of the gap is remotely realized by means of a dilatation system. Laser Doppler Vibrometry (LDV) is used to measure the transverse displacement of the sample rod in three different conditions: in air, in stagnant water and under turbulent axial flow rate. In this paper we detail the design criteria of the experience and measurement principle to then focus on the experimental program and its results are discussed.

**Index Terms**—Nuclear, Instrumentation, Measurement, Test Bench, fuel rod, PCMI, dynamics, vibrations, LDV

## I. INTRODUCTION: BACKGROUND AND OBJECTIVES

**T**HROUGH the past years, Pellet-Cladding Mechanical Interaction (PCMI) has constituted an issue in the definition of technical specifications for the operation of nuclear power plants and for the identification of associated safety

Manuscript received xxx.

V. D’Ambrosi, C. Destouches and S. Breaud were with the CEA, DEN, DER, Instrumentation Sensors and Dosimetry Laboratory, Cadarache, F-13108 St Paul Lez Durance, France. (email veronica.D’AMBROSI@cea.fr)

G. Ricciardi was with CEA Cadarache - DEN/DTN/STCP/LTHC, 13108 Saint Paul Is Durance, France

F. Lebon was with Aix Marseille Univ, CNRS, Centrale Marseille, LMA, Marseille, France

J.M. Gatt, J. Julien and D. Parrat were with DEN/DEC, French Alternative Energies and Atomic Energy Commission (CEA) F- 13108 St-Paul-lez-Durance - France

margins. Consequently, research has attempted to improve the knowledge of this complex phenomenon by numerical simulations, developing multi-physics models, and by experiments in Material Testing Reactors (MTR) [1]. In the latter, environmental constraints have strongly limited the possibility to obtain real time measurements and thus to allow the characterization of the kinetics phenomenology. At present days, a need for highly instrumented experiences in MTRs and for on-line measurements to gain real time data during irradiation has been expressed.

ADELINÉ is a specific irradiation device designed for the next future JHR. PWR temperature and pressure conditions are reproduced in the device and it will be partially dedicated at studying PCMI.

In this frame we have identified relevant and measurable parameters associated to PCMI during normal irradiation and incidental conditions. We also proposed a model to characterize fuel material behavior undergoing initiating central melting in the attempt at evaluating its macroscopic impact on PCMI [2]. We are working to propose innovative and efficient measurement methods for detecting and characterizing this complex multi-physics phenomenology. Among the identified relevant parameters, vibrations distinguished as a possible application case.

Flow Induced Vibrations (FIV) of nuclear fuel rods in axial turbulent flow rate have been concerned by a large variety of scientific studies. According to Païdoussis [3] [4] and Axisa [5] flow induced vibrations come from two mechanisms: the drag force in the turbulent boundary layer near the structure (near-field component) and from the wall pressure fluctuations and far field noise. They generally induce transversal vibrations of small amplitudes, typically the vibration amplitude  $y/D_c$  does not exceed  $10^{-3}$ ,  $y$  being the r.m.s. amplitude of vibration and  $D_c$  the cylinder diameter. In the nuclear field, works are mainly motivated by fretting concern, phenomenon appearing at the grid-rod interface.

Few researches have been carried out on the effects of non linear mechanisms arising from the presence of pellets within the fuel rod. It is generally argued that modeling those effects is rather difficult [6]. Benhamadouche in [7] proposed to evaluate an equivalent mass density for the rod which accounts for the presence of pellets. This density is then used in the evaluation of the dynamic behavior of the fuel rod taken as a linear Euler Bernoulli beam. Park and al. in [8] make the point on the fact that since a gap exists between pellets and gap, the contribution of the pellet mass to the density for dynamic

evaluation cannot be clearly determined. They propose to compare the natural frequencies of empty and fulfilled rods to estimate an appropriate density. The fuel rod vibration is then evaluated, still assuming a linear behavior.

The non linear vibration of fuel rod has been recently studied by Ferrari and al. [6]: his study concerned a 900 mm zircaloy clad, clamped at both extremities, eventually fulfilled with cylindrical tungsten carbide pellets modeling uranium fuel pellets in terms of dimensions and density.

They compared the dynamics of empty rod, fulfilled rod freely moving (no spring at one bottom of the fuel column) and fulfilled rod axially constrained in air and in quiescent water. They observed that pellets decrease natural frequencies of the rod and that axial constriction increases natural frequencies and reduced damping with respect to freely moving configuration, both in air and in water. Moreover, they stated that non linear mechanisms were experimentally observed during tests. No studies have been retrieved discussing the effect on the dynamics of the fuel rod of local pellet-clad contact due to gap closure.

The unknown, non linear behavior of the system implies that predictively model the system cannot lead to a reliable evaluation of the feasibility of characterizing PCMI through its impact on rod dynamics. This justified the design of the experimental set up IMPIGRITIA<sup>1</sup>. The system has been designed to be representative of the geometry of ADELIN irradiation device and to recreate the turbulent axial excitation. The experimental program has been carried out in two phases: a first test phase in air leads to state the feasibility of measuring the phenomenon under laboratory conditions and to identify a correlation between the axial extension of PCMI and the effect on rod dynamic response. The second phase, under axial turbulent excitation allows to define whether FIV are sufficient to have a passive measurement and what is the impact of flow rate on the feasibility of the measure.

This paper is structured as follows: we briefly proceed in the next section II with the numerical approach developed to describe the system, highlighting the empirical parameters to be measured and proposing a linear approximation of the problem as a support for the design phase. Section III is then dedicated to the measurement principle. We proceed to section IV which is devoted to the design criteria of the experimental set-up. Section V then briefly describes the set up, details the instrumentation used and rod configurations. In section VI we first present the comparison between experimental measures results by linear approximation. Then we discuss the results of air tests meant at demonstrating the feasibility of the measure in controlled conditions. The experimental evidence of a modification in the dynamic behavior of the rod depending on PCMI shall motivate the realization of the second phase of the experimental campaign to prove the feasibility of the measure under passive FIV representative of ADELIN irradiation device in JHR. Conclusions and further work are presented in section VII.

<sup>1</sup>Acronym form "Interaction Mécanique Pastille Gaine : Réalisation du Test vIbratoire", from *latin* impigritia, impigritiaie; means "zeal, dedication"

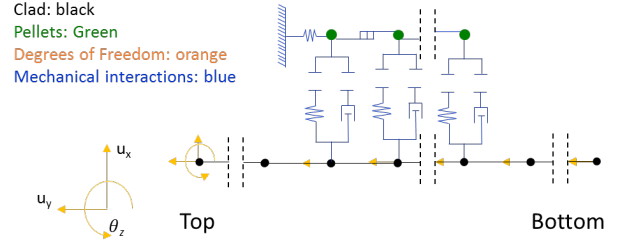


Fig. 1: Numerical model of IMPIGRITIA: schematic view of the configuration

## II. THE NUMERICAL APPROACH

### A. Definition of the model

Figure 1 shows a schematic view of the proposed model. The sample holder and the empty clad are modelled as a cantilevered Euler-Bernoulli beam by a 2D finite element model. Each node of the clad can move along the radial ( $u_x$ ) and the axial direction ( $u_y$ ) and can rotate ( $\theta_z$ ). Pellets are considered as discrete masses  $m_p$  interacting along the radial direction with corresponding clad nodes through the non linear mechanism of dissipative shock and with each other through Coulomb friction. The equation of motion to be solved is [9]:

$$[M]\{\ddot{x}\} + [C]\{\dot{x}\} + [K]\{x\} + \{f_{nl}\} = \{F_e\} \quad (1)$$

Where  $[M]^{N,N}$  is the total mass matrix,  $[C]^{N,N}$  the total damping matrix,  $[K]^{N,N}$  the total stiffness one. They are obtained as follows:

$$[M] = \begin{bmatrix} [M_c] & 0 \\ 0 & [M_p] \end{bmatrix} \quad [C] = \begin{bmatrix} [C_c] & 0 \\ 0 & [C_p] \end{bmatrix} \quad (2)$$

$$[K] = \begin{bmatrix} [K_c] & 0 \\ 0 & [K_p] \end{bmatrix}$$

where  $[M_c]^{n,n}$  is the tridiagonal mass matrix for the clad and  $[M_p]^{m,m}$  is the diagonal mass matrix for the pellets, with  $N = m + n$ . In the same way the total stiffness matrix and the total damping one depends on clad and pellets ones.

Rayleigh damping is used to model the damping matrix [C]:

$$[C] = \alpha[M] + \beta[K] \quad (3)$$

Assuming proportional damping, the dissipation in the structure can be described by two parameters  $\alpha$  and  $\beta$ . Those parameters, which are not a priori known, are experimentally determined measuring the first two eigen-frequencies of the system in air. Indeed it can be shown that [10]:

$$\zeta = \frac{1}{2} \left( \frac{\alpha}{\omega_i} + \beta\omega_i \right) \quad (4)$$

where  $\zeta$  is the modal damping, which can be recovered by logarithmic decrement from free damped vibrations of the system and  $\omega_i$  are the eigen-frequencies.

The non-linear forces acting on the system are expressed by the  $\{f_{nl}\}$  term in equation (1). Those forces are the dry friction

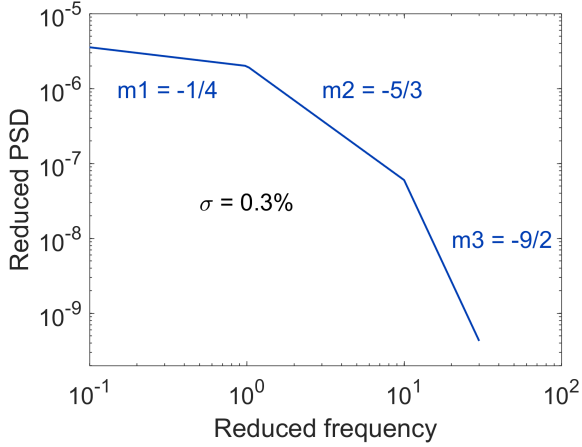


Fig. 2: Reduced PSD of wall pressure fluctuations [5]

between discretized pellet nodes and the shock interaction between pellet nodes and clad ones. Gap size is a parameter in the formulation of pellet-clad shock interaction.

The presence of external water plays a role in the external solicitation  $\{F_e\}$  but it also induces an additional viscous damping to the structure: according to De Pauw in [11] the effects of flowing fluid on the spectral response of the structure is described by an added mass  $m_a$ , corresponding to the mass of displaced fluid, and a dynamic amplification factor  $C_m$  such that:

$$f = \frac{1}{2\pi} \sqrt{\frac{K}{M + C_m m_a}} \quad (5)$$

where  $K$  and  $M$  are the structural stiffness and mass of the system. The dynamics amplification factor is equal to 1 for quiescent water thus the two parameters can be experimentally obtained by comparing the oscillation frequencies of the system in air, in quiescent water and in fluid flow.

The external force  $\{F_e\}$  corresponds to the drag force and wall pressure fluctuations present in the fluid flow rate. According to the statistic approach proposed by Axisa [5] on the basis of the study done by Clinch [12], the reduced ‘‘Power Spectral Density PSD’’ of the  $\{F_e\}$  is in the form:

$$P\tilde{S}D(f_r) = P\tilde{S}D(f_{r0}) \left( \frac{f_r}{f_{r0}} \right)_i^m \quad (6)$$

where  $P\tilde{S}D$  is obtained by dividing the PSD by  $\rho_0^2 v_0^3 D$  with  $\rho_0$  the fluid density,  $v_0$  the fluid velocity and  $D$  the characteristic dimension of the problem (in this case the hydraulic diameter).  $f_r = \frac{fD}{v}$  is the reduced frequency while  $m_i$  is detailed in figure 2.

To solve the equation, explicit Newmark scheme has been implemented. As reported in [9] direct time integration is necessary when the problem is non linear in order to avoid strong dependencies of results on integration time step.

### B. Investigation of parameters: an empirical model

The displacement  $\{x\}$  of the structure, obtained when solving motion equation (1) by mean of explicit Newmark

integration scheme, can be expressed as a function of the set of parameters  $\mathbb{P}$ , resulting from the previous discussion:

$$\{x\} = f\{\mathbb{P}\} = f\{\mathbf{M}_p, \mathbf{M}_c, m_a, C_m, \mathbf{K}_p, \mathbf{K}_c, \alpha, \beta, K_{co}, C_{co}, \mu, j, v^2\} \quad (7)$$

where  $\mathbf{M}_i$ ,  $\mathbf{K}_i$ ,  $\alpha$  and  $\beta$  have already been defined,  $m_a$  and  $C_m$  are the added mass and the dynamic amplification factor due to the fluid presence and fluid flow.  $K_{co}$  and  $C_{co}$  are the parameters characterising the pellet-clad shock interaction, modelled through a contact stiffness  $K_{co}$  and a viscous dissipation  $C_{co}$  [13];  $\mu$  is the friction coefficient to model the pellet-pellet interaction.  $j$  is the width of the gap and  $c$  is the fluid velocity.

While some of those parameters are completely defined by the geometry of the structure (i.e. the mass matrix of pellets  $\mathbf{M}_p$  and sample holder  $\mathbf{M}_c$ , the stiffness matrix of the sample holder), the others have to be experimentally determined. Identification of model parameters adapted to fit at best experimental data allows calibration of the model. They are resumed in table I.

TABLE I: Model parameters

Parameter	Description
$K_p$	Pellet Stiffness
$\zeta(\alpha, \beta)$	Modal damping
$m_a$	Added mass
$C_m$	Dynamic amplification factor
$K_c$	Contact Stiffness
$C_c$	Contact viscous dissipation
$\mu$	Pellet-Pellet Friction Coefficient
$j$	Pellet-clad gap
$v$	Fluid velocity

### C. The linear approximation

A simplified approach can be used to dimension the heterogeneous system behavior in terms of expected frequencies and modes of vibration by neglecting the non linear interactions  $\{fnl\}$ .

$$[M_{eq}]\{\ddot{x}\} + [C_{eq}]\{\dot{x}\} + [K_{eq}]\{x\} = \{F_e\} \quad (8)$$

In this case we assume the bending stiffness to be given only by the geometry and inertia of the clad and the sample holder  $[K_{eq}] = [K_c]$ . Pellets contribute instead to the linear mass of the system  $[M_{eq}]$ . The damping matrix of the simplified system is a function of the equivalent mass, of sample holder and clad stiffness through Rayleigh (eq. 3):

$$[C_{eq}] = \alpha[M_{eq}] + \beta[K_{eq}] \quad (9)$$

Validation of this approach is presented in section VI-B

### III. THE MEASUREMENT PRINCIPLE

Mechanical dissipations, as already mentioned, arise from the presence of pellets inside the clad [6]. The progressive closure of the radial gap along rod axis limits those effects and changes the behavior of the system: a reduction in structural damping as a consequence of the decrease in dissipative mechanisms is expected. A slight decrease in its eigenfrequencies could arise. Those variations can be retrieved by measuring the displacement amplitude of the system  $x(t)$ .

#### A. Free vibration tests

During free vibration tests, viscous damping ratio is obtained by an adaptation of the logarithmic decrement method, the "Consecutive Logarithmic Decrement Method" C-LDM as described by Heitz in [14].

We recall that the viscous damping for an under-damped linear "Single Degree Of Freedom" SDOF system can be obtained by "Logarithmic Decrement Method" LDM measuring its displacement along time. The displacement can be written in the following form:

$$x(t) = \exp(-\zeta\omega_0 t) (A \cos(\omega_d t) + B \sin(\omega_d t)) \quad (10)$$

where  $\omega_0 = 2\pi f_0$  is the natural frequency of the SDOF system,  $\omega_d = \omega_0 \sqrt{1 - \zeta^2}$  is the pseudo-angular frequency which is directly measured by the pseudo-period  $T_d$ ,  $A$  and  $B$  depend on the initial conditions of the problem, as presented in figure 3. The term  $\exp(-\zeta\omega_0 t)$  describes the decay of free oscillations. In this case, to obtain the viscous damping ratio  $\zeta$  it is sufficient to consider two different local maxima: considering the peak displacement  $x_i$  occurring at time  $t$  and the peak displacement  $x_{i+n}$  at time  $t + nT_d$ :

$$\frac{x_i}{x_{i+n}} = \frac{\exp(-\zeta\omega_0 t)}{\exp(-\zeta\omega_0 (t + nT_d))} = \exp(\zeta\omega_0 nT_d) \quad (11)$$

For non linear viscous damping phenomenon the "Consecutive LDM" C-LDM adapted method can be applied: two successive local maxima are considered and the viscous damping ratio is evaluated  $N$  times. The viscous damping ratio is a function of displacement amplitude due to non linearities in the system.

#### B. Forced vibrations tests

Under the turbulent fluid flow rate excitation the system undergoes forced vibrations and the characterization is to be carried out in the frequency domain through Fourier transform.

$$X(\omega) = \mathcal{P}[x(t)] = \int_{-\infty}^{\infty} x(t) e^{-i\omega t} dt \quad (12)$$

Making the hypothesis that the low-level dynamic excitation lead us to assume a linear behavior of the system, the "Half-power bandwidth" method HBM can be applied: taking the transfer function of the measured displacement with respect to the external applied force as taken from Axisa [5], we are able to locally fit a dynamic displacement amplification factor in the following form:

$$|H_d(\omega)| = \frac{1}{\sqrt{\left(1 - \left(\frac{\omega}{\omega_0}\right)^2 + \left(2\zeta\frac{\omega}{\omega_0}\right)^2\right)}} \quad (13)$$

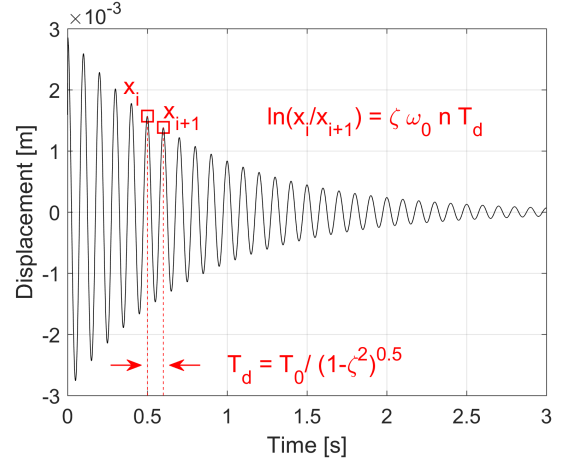


Fig. 3: Principle for the LDM for under-damped free vibrations of a SDOF system

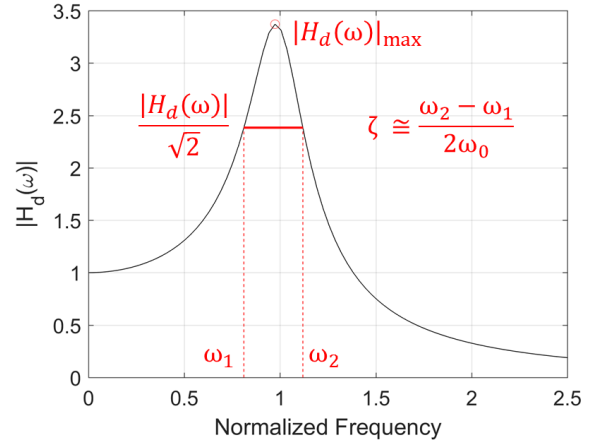


Fig. 4: Principle for the HBM for under-damped free vibrations of a SDOF system

From this the viscous damping ratio can be estimated as

$$\zeta \cong \frac{\omega_2 - \omega_1}{2\omega_0} \quad (14)$$

where  $\omega_2$  and  $\omega_1$  are the frequencies for which  $|H_d(\omega_1)| = |H_d(\omega_2)| = \frac{|H_{d,max}|}{\sqrt{2}}$ . The general method is represented in figure 4.

### IV. DESIGN CRITERIA: THE REPRESENTATIVENESS ISSUE

ADELIN [15] is a 4m high irradiation device and constitutes the evolution of ISABELLE 1 system as it was in OSIRIS reactor [16]. As its predecessor, it presents a single rod test section where temperature and pressure conditions characteristics of a PWR are reproduced (155 bar and 275°C inlet water temperature). The tested rod has the geometry of a FABRICE type fuel-rod [16]: a short element (about 60 cm in length) obtained cutting a previously irradiated 4m long fuel rod to be adapted to MTR geometry. The rod is cooled by an up-streaming turbulent flow rate. It is maintained in the section by a sample holder and centered by four centering elements. In order to be representative of ADELIN configuration,

we accounted for the real environmental conditions, for the geometrical design, material characteristics and hydraulic solicitation.

### A. The environment

Thermal and mechanical properties are obviously impacted by the environmental conditions but, through the years, several correlations have been developed to account for these phenomena [17]. Those correlations will be used during post-treatment of results to establish the attended behavior in PWR conditions.

The pressurization of the circuit has no impact on the vibration of the component, thus leading to design a low pressure system.

### B. The geometry

Mechanical similarity and scale reduction cannot simply be applied and a full scale system implied non negligible conception, exploitation and cost issues. Still, geometry and fixation conditions strictly impact the dynamics of a structure thus the clamped free conditions of ADELIN sample is maintained in the experimental set-up.

ADELIN sample holder is made of an upper part and a lower part, the sample rod is screwed on the lower part of the sample holder and centered in the experimental section by mean of four centering elements. The upper and lower parts are coupled by a mechanical system. We decided to limit our study to the lower part of sample holder. The decision lead to an experimental system of about 1.5 m and the choice is expected to strengthen the impact of a local pellet-clad interaction on the global dynamics of the structure.

The shortening of axial extension induces a reduction in the stiffness of the system, leading to an increase in the eigenfrequencies of the system. Table II resumes the first six expected eigenfrequencies  $f_{i,l}$  for ADELIN and IMPIGRITIA, obtained according to the linear approximation described in section II-C.

TABLE II: Eigen-frequencies of ADELIN and IMPIGRITIA devices by linear approximation. Frequencies are reported in Hz

Device	$f_{1,l}$	$f_{2,l}$	$f_{3,l}$	$f_{4,l}$	$f_{5,l}$	$f_{6,l}$
ADELIN	1.5	7.6	13.0	21.6	42.6	65.1
IMPIGRITIA	6.2	29.0	79.9	170.2	261.9	343.0

### C. The hydraulic similarity for FIV

Fuel rod to be installed in the ADELIN device will be submitted to a turbulent flow rate of approximately 1 m/s at about 275°C and 155 bar along the axial direction, from the bottom to the top. Hydraulics is dimensioned in order to reproduce the external solicitation in terms of the axial turbulent flow and pressure fluctuation in the flow. We identified a range of representativeness first by imposing the conservation of wall pressure fluctuations and secondly applying the Burgreen

principle [18]. The conservation of wall pressure fluctuation  $p_{rms}$  was imposed according to the definition proposed by Axisa in [5] on the basis of the envelop PSD derived from Clinch data [12] and reported in equation (15). The simulation criterion established by Burgreen instead has been recently used by De Paw et al. in [11] to study flow induced vibrations in a prototype representative of the MHYRRA system and it is reported in equation (16).

$$p_{rms} = 0.003(\rho v^2) \quad (15)$$

where  $p_{rms}$  is the root mean square of pressure fluctuations,  $\rho$  is fluid density and  $v$  is average flow velocity.

$$v_{exp} = v \frac{\rho^{0.5} \mu^{-0.33} E^{-0.33} M^{0.165}}{\rho_{exp}^{0.5} \mu_{exp}^{-0.33} E_{exp}^{-0.33} M_{exp}^{0.165}} \quad (16)$$

Subscript 'exp' stands for prototype,  $\mu$  the fluid dynamic viscosity,  $E$  elastic modulus and  $M$  the mass of the sample rod at operating temperature.

Applying the described criteria in our test conditions we found a range of representative flow rate. Fluid flow velocity ranges between 0.9 to 2.6 the fluid velocity at the sample rod in ADELIN.

$$\frac{v_{exp}}{v} \in [0.9 : 2.6] \quad (17)$$

## V. THE EXPERIMENTAL SET-UP

For the experience, several representative hollow zircaloy clads were supplied. As previously mentioned, the geometrical configuration of the sample rods was defined on the basis of the FABRICE type fuel rods used in ADELIN: the zirconium alloy clad has an external diameter of 9.5 mm and its material properties are reported in table III. We defined a length coherent with the FABRICE characteristics, thus 550 mm long. Each side is welded to a plug which is screwed on a prolongation tube in stainless steel.

The prolongation tube constitutes the sample holder and it is fixed at the top of the experimental section. The other side is instead free to move. A simplified scheme of the sample holder is presented in figure 5.

Due to environmental and realization issues, the  $UO_2$  constituting the real fuel material was replaced by cylindrical Molybdenum pellets. A comparison of room temperature material properties of  $UO_2$  and Mo are resumed in table III. Pellets diameter was defined according to standard radial dimension of  $UO_2$  fuel pellets, the height instead was deduced by mass conservation of  $UO_2$  fuel pellets.

In order to fulfill the fabrication gap existing between pellets and clad and remotely control PCMI, a dilatation system capable of local expansion is used. It has been developed for

TABLE III: Material properties of interest at  $T_{AMB}$

Material	Density [kg/m <sup>3</sup> ]	Young's Modulus [GPa]
Zircaloy	6570	95
$UO_2$	10963	194.3
Mo	10200	320



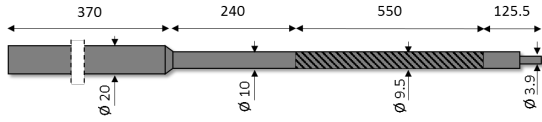


Fig. 5: Sample holder scheme: the dashed region indicates the fictive fuel rod position

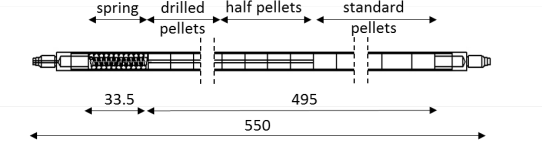


Fig. 6: Fuel rod scheme: in order to allow positioning the dilatation system from the top of the rod to the central region, top pellets are drilled and where PCMI is wanted pellets are replaced by two half-pellets.

stent implantation in the medical domain and it is made of a balloon which expands once inflated. The system is remotely controlled by a connection tube. A general assembly scheme is presented in figure 6: the component is introduced from the top of the sample holder, through centrally drilled pellets and the balloon is placed in the region where gap closure wants to be induced. There, pellets are replaced by two half pellets, which are displaced by mean of the previously described dilatation of the system, leading to pellet-clad contact.

Different rod configurations were tested to identify the minimum number of contacting pellets leading to a measurable effects. For this we used balloons having different lengths. Rod configurations are resumed in table IV. To calibrate the model and characterize system dynamics response, two other rods were manufactured: an empty rod **C0** to characterize modal parameters governing the linear dynamic response of the sample rod and **C6**, where Mo pellets and clad are designed to stick together. This last configuration allows to measure the effect due to a complete closure of the gap on sample rod dynamics. We also manufactured **C1** fuel rod with standard Mo pellets which allows to highlight possible bias due to the presence of dilatation system. We wont present this last study, rather focusing on the first objective of the experience: to demonstrate the possibility of measuring a first pellet-clad contact through a modification in system dynamics.

Vibration data of the sample rod are collected through a Laser Doppler Vibrometer (LDV) system: the laser beam is pointed on the vibrating object and scattered back from it. The velocity and displacement amplitudes of the studied object generate a frequency or a phase modulation respectively, due to Doppler effect. The laser used is a class 2 Helium-neon type, having a wavelength of 633 nm and a cavity length of 204 +/- 1 mm. Located at about 0.5 m from the moving rod, the spot on the rod is about 50  $\mu\text{m}$ . The experimental section is completely designed in optical quality plexiglass. It has been demonstrated by De Pauw et al in [19] that LDV technique leads to a higher signal-to-noise ratio than other measurement techniques

TABLE IV: Rod configurations

Rod name	N° of displaced pellets	Axial extension of gap closure
C0	No pellets	none
C1	0	0 mm
C2	1	15 mm
C3	3	45 mm
C4	5	75 mm
C5	9	135 mm
C6	0	495 mm

TABLE V: Instrumentation

Parameter	f [Hz]	Instrument	Accuracy ( $1\sigma$ )
frequency	$10^4$	Laser Doppler Interferometer	0.1 Hz
Temperature	1	K type thermocouples	+/- 1.5 K
Pressure	1	pressure gauges	+/- 0.3 bars
Flow rate	imposed	Vortex effect flow meter	+/- 2 l/min

as grid method, fiber Bragg grating sensors, electrical strain gauges and accelerometers.

To produce and control flow conditions in the experimental section we have designed a dedicated independent water loop, equipped with a circulation pump, an expansion tank and a cooling system to keep temperature constant in the system during tests. All conditioning components are located on a separate frame to limit noise effect on LDV measures. To monitor conditions in the circuit we have installed a flow meter at the experimental section inlet, three thermocouples located at different positions to verify temperature evolution in the loop and three pressure gauges to check pressure drops. A summary of instrumentation characteristics and accuracy is reported in table V.

## VI. FEASIBILITY IN AIR

During the experience we were not able to assess the evolution of C4 and C5 due to unforeseen experimental events. Water fulfilled the rods leading to the impossibility to observe any modification depending on gap closure. As a consequence we cannot identify a clear correlation between the number of attached pellets to the clad and the modification in system behavior. Anyway the main object of the experience is to state the feasibility of measuring first contacts between pellets and clad, which is possible analyzing the behavior of the other rod configurations. Free vibration tests were carried out in air, maintaining the same fixation conditions of flow rate tests and imposing an initial displacement to the fixed-free system, exciting the first vibration mode. Oscillations were measured at the bottom end of the rods, where displacements amplitudes were the highest.

### A. Data Processing

We collected the displacement and velocity of the moving rod at a sampling frequency of 10 kHz. Test was repeated N times for each rod configuration. The dilatation system was inflated at 8 bars, internal pressure which guarantees the local

disappearance of relative motion of pellets. We apply to the measured signal a low pass Butterworth filter with a cutting frequency of 5 kHz. As previously described, the C-LDM is used to evaluate the decay of viscous damping ratio of the  $i_{th}$  measurement. We then evaluate the average evolution and data dispersion for each rod. To obtain the frequency, DFT is applied, evaluating it according to Hanning type windowing, with a superposition of 0.5.

### B. Validation of the linear approximation method

We compare collected data for the C0 and C6 rod with the linear approximation of the system as described in section II-C. The absence of the dissipative mechanisms coming from the gap presence and relative motions of the pellets with respect to the clad is expected to lead to a linear behavior of the two rod configurations.

1) *The empty rod (C0):* For the specific case we have:

$$[M_{eq}] = [M_c] \quad [C_{eq}] = [C_c] \quad [K_{eq}] = [K_c] \quad (18)$$

We impose viscous damping ratio  $\zeta$  by evaluating the average value from air tests and assuming a linear behavior of the empty rod. Figures 7 shows the comparison between calculated and measured displacement of the moving rod in time and frequency domain. The experimental and calculated first mode eigen-frequencies of the system correspond, with a relative variation smaller than the accuracy of the LDV system.

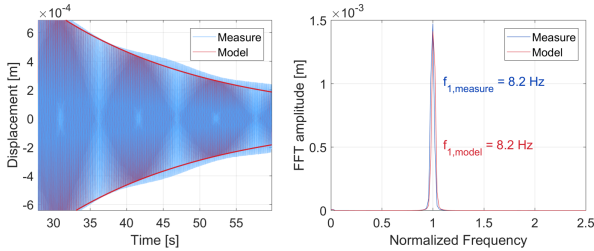


Fig. 7: Comparison of calculated and measured behavior for the C0 rod configuration: time evolution of the displacement (left) and first eigen-frequency (right)

On the other hand we can observe that the empty rod does not present a perfectly linear behavior. This is better highlighted in figure 8. Here we have in light blue the  $\zeta$  obtained by C-LDM method and in dark blue the mean value obtained by moving average. Comparing it with the global mean value imposed in the model, we have that relative variation can locally reach 50% in the region from  $x_{RMS} = [10^{-4} : 7.10^{-4}]$  mm to increase to 80% at smaller displacement amplitudes. This increase in the relative variation of the estimation comes from an experimental bias of the measure characteristics of all air measurements.

It results that the linear approximated method is not adapted to model the dynamics of the rod, especially in the region  $x_{RMS} < 2.10^{-4}$  which corresponds to the range of transversal displacement expected in ADELINÉ, when submitted to FIV. The non linear model is thus necessarily to correctly model system behavior.

2) *The closed gap rod (C6):* In this case we assumed only pellets to contribute to the mass of the rod while the stiffness of the clad is the one of a full rod having the external diameter of the original clad, thus 9.5 mm. As done for the empty rod, the viscous damping ratio  $\zeta$  is determined by taking the global mean value experimentally obtained.

As shown in figure 9 the frequency of the first mode is evaluated with an accuracy comparable to the one of the measurement system.

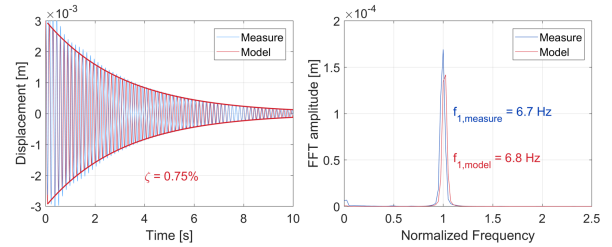


Fig. 9: Comparison of calculated and measured behavior for the C6 rod configuration: time evolution of the displacement (left) and first eigen-frequency (right)

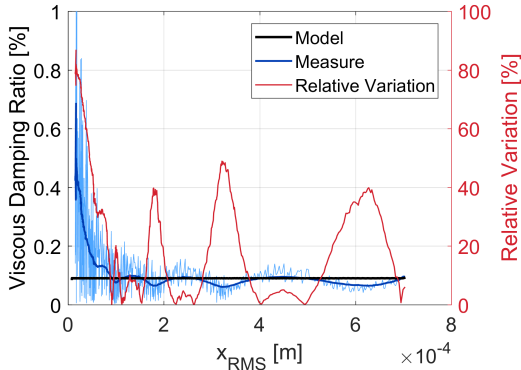


Fig. 8: Relative variation in viscous damping decay as a function of rms displacement amplitude.

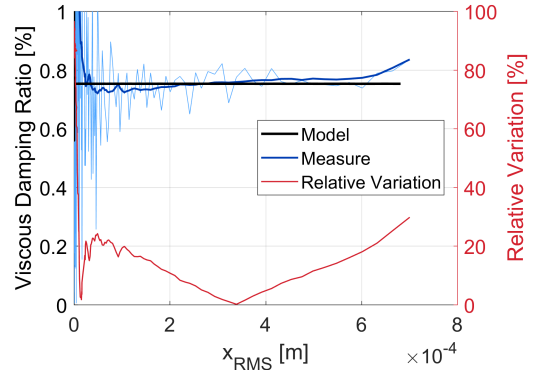


Fig. 10: Relative variation in viscous damping decay as a function of rms displacement amplitude.



Figure 10 presents the result of C-LDM for the full rod: in this case the much more linear behavior of the rod leads to keep the relative error smaller than 30% along the examined region.

### C. Technological feasibility of the measure

1) *Modification of the frequency of the first mode:* Table VI resumes the experimental results about first mode eigen-frequency for the rod configurations under analysis and depending on PCMI interaction for rods allowing it (C2 and C3). No variation in frequency was observed during the experience for both fuel rod configurations C2 and C3 depending on the local closure of the gap. Difference in frequencies for the C1, C2 and C3 configurations lies within the precision of the LDV system ( $\pm 0.1$  Hz). C6 shows a slightly higher frequency for the first mode, coming from an increase in the global stiffness of the geometry. Indeed by linear approximation we obtained a first mode eigen-frequency with a precision of 0.1 Hz, as mentioned in the previous section VI-B.

TABLE VI: Experimental frequencies for the different rod configurations

Rod configuration	$f_{1,open}$ [Hz]	$f_{1,closed}$ [Hz]
C0	8.2	none
C1	5.7	none
C2	5.8	5.8
C3	5.7	5.7
C6	6.7	none

2) *Modification of the decay of free vibrations:* Figure 11 shows the decay of the viscous damping ratio for the C3 rod configuration and corresponding data dispersion. We recall that C3 presents 3 couples of half pellets leading to the possibility of inducing gap closure over 45 out of 495 mm of the axial length of the “fuel” column.

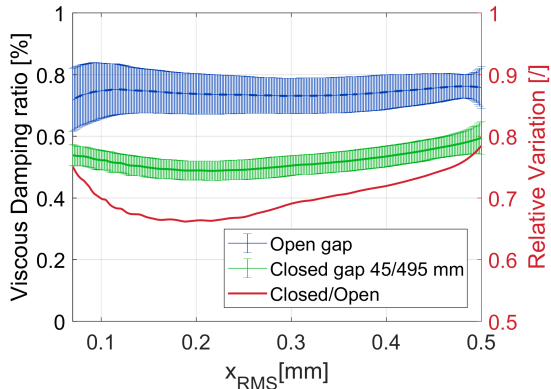


Fig. 11:  $\zeta$  evolution along the amplitude of displacement for C3 rod, in blue the open gap configuration, in green after inflation of the dilatation system leading to local closure of the gap. In red the relative variation

According to what we expected, the local closure of the gap leads to a decrease in the viscous damping ratio: the system

vibrates more due to a decrease in the internal dissipation mechanisms: pellet-clad shocks are reduced as a consequence of the disappearance of the radial gap. The relative variation ranges from a maximum decrease of 35% to a minimum one of about 20% and is clearly measurable even in the region of representative displacement of ADELIN device  $x_{RMS} < 2.10^{-4}$ .

To better characterize the non linear interactions leading to this reduction, further work is being done to study system behavior by the non linear model presented in section II. This experimental result positively states on the possibility to measure the impact on rod dynamics due to a local closure of pellet-clad gap and motivates the further study under FIV.

## VII. CONCLUSIONS AND FURTHER WORK

The IMPIGRITIA test bench was designed to investigate PCMI and innovative measurement methods. The experiment was designed to verify whether a modification can be measured in the frequency or in the vibration damping of the system as a function of a local gap closure. The relative motion of pellets against the clad depends on the relative motion between the two, which is a function of the gap extension. When gap disappears due to pellet-clad attachment, the dissipation is meant to disappear, thus leading the system to longer oscillations.

Different rod configurations were manufactured to verify the possibility of observing a progressive reduction in damping and modification in frequency depending on the axial extension of pellet-clad contact. This was obtained in controlled conditions by remotely inflating a dilatation system which leads to gap closure. Experimental unforeseen events lead to the impossibility to characterize the dynamic behavior of rod configurations having the highest number of pellets attached to the clad (C4 and C5). The assessment of the other rods still gave us the possibility to verify the impact of a first contact between pellets and clad on system dynamics, which is the main objective of this work.

The experimental program presented a first phase of air characterization of the structure, whose geometry is designed to be representative of the ADELIN sample holder. Air tests were carried out in free vibrations conditions, imposing an initial displacement to the structure and measuring the decay of oscillations as a function of displacement amplitude. Experimental results highlighted the limits of linear approximation method. We are working for the further development of the non linear modeling.

This phase allowed to positively state on the feasibility of measuring PCMI through vibrations under controlled conditions. Even though no variations in frequency were observed, the analysis of the decay of the free vibrations of C3 lead us to observe that a modification is induced by the local closure of the gap. The gap closure over 45/495 mm induced a clear reduction in the viscous damping ratio of the structure, ranging from a reduction of 20% to 35%. This difference was clearly visible also in the region of displacement amplitude representative of the FIV in the ADELIN device. Following the results of air tests, we are currently analyzing measures

obtained in the second test phase. In this phase, different rod configurations were tested under turbulent fluid flow rate to prove measure feasibility under passive FIV representative of the real application case. Depending on the results of such analysis, we shall proceed to propose a technological solution adapted to the environmental and geometrical burdens of the real irradiation device ADELIN inside the JHR nuclear research reactor.

## REFERENCES

- [1] B. Michel, J. Sercombe, C. Nonon, F. Michel, and V. Marelle, "Simulation of Pellet-Cladding Interaction with the PLEIADES Fuel Performance Software Environment," *Nuclear Technology*, vol. 182, pp. 124–137, 2013.
- [2] V. D'Ambrosi, J. Gatt, F. Lebon, J. Julien, D. Parrat, and C. Destouches, in *Proceedings of MECAMAT 2018*, 2018.
- [3] M. P. Paidoussis, *Fluid-Structure Interactions, Slender Structures and Axial Flow*. ELSEVIER, 2004, vol. 2.
- [4] M. P. Paidoussis, "Fluidelastic vibration of cylinder arrays in axial and cross flow: State of the art," *Journal of Sound and Vibration*, vol. 76, no. 3, pp. 329–360, 1981. [Online]. Available: <http://www.sciencedirect.com/science/article/pii/0022460X81905162>
- [5] F. Axisa, *Modélisation des systèmes mécaniques : Vibrations sous écoulements*. Hermes, 2001, vol. 4.
- [6] G. Ferrari, P. Balasubramanian, and al., "Non-linear vibrations of nuclear fuel rods," *Nuclear Engineering and Design*.
- [7] S. Benhamadouche and al., "CFD estimation of the flow induced vibrations of fuel rod downstream a mixing grid," *proceeding of the ASME 2009 Pressure vessels and Piping division conference*.
- [8] N. Park, H. Rhee, J.-K. Park, S.-Y. Jeon, and H.-K. Kim, "Indirect estimation method of the turbulence induced fluid force spectrum acting on a fuel rod," vol. 239, no. 7, pp. 1237–1245. [Online]. Available: <http://www.sciencedirect.com/science/article/pii/S0029549309001320>
- [9] M. Gradin and D. J. Rixen, *Mechanical Vibrations, Theory and Application to Structural Dynamics.*, third edition ed. Wiley.
- [10] A. Alarcon, "Code aster: Modeling of damping in dynamics linear."
- [11] B. De Pauw, W. Weijtjens, S. Vanlanduit, K. Van Tichelen, and F. Berghmans, "Operational modal analysis of flow-induced vibration of nuclear fuel rods in a turbulent axial flow," *Nuclear Engineering and Design*, vol. 284, pp. 19–26, Apr. 2015. [Online]. Available: <http://www.sciencedirect.com/science/article/pii/S0029549314006694>
- [12] J. M. Clinch, "Measurements of the wall pressure field at the surface of a smooth-walled pipe containing turbulent water flow," *Journal of Sound and Vibration*, vol. 9, pp. 398–419, 1969.
- [13] P. Wriggers, *Computational Contact Mechanics*, second edition ed. Springer Berlin Heidelberg New York.
- [14] T. Heitz, "Nonlinear local behaviours and numerical modeling of damping in civil engineering structures in dynamic," Ph.D. dissertation, Universit Paris-Saclay, 2017.
- [15] C. Gonnier, J. Estrade, G. Bignan, and B. Maugard, in *Proceedings of IGORR 2017*, 2017.
- [16] A. Alberman, M. Roche, P. Couffin, S. Bendotti, D. Moulin, and J. Boutfroy, "Technique for power ramp tests in the isabelle 1 loop of osiris reactor," *Nuclear Engineering and Design*, vol. 168, no. 1, pp. 293–303.
- [17] J. K. Fink, "Thermophysical properties of uranium dioxide," vol. 279, pp. 1–18.
- [18] V. Prakash, M. Thirumalai, M. Anandaraj, P. A. Kumar, D. Ramdasu, G. Pandey, G. Padmakumar, C. Anandbabu, and P. Kalyanasundaram, "Experimental qualification of subassembly design for prototype fast breeder reactor," vol. 241, no. 8, pp. 3325–3332. [Online]. Available: <http://linkinghub.elsevier.com/retrieve/pii/S0029549311003487>
- [19] B. D. Pauw, S. Vanlanduit, K. V. Tichelen, T. Geernaert, K. Chah, and F. Berghmans, "Benchmarking of deformation and vibration measurement techniques for nuclear fuel pins," pp. 3647–3653. [Online]. Available: <https://reader.elsevier.com/reader/sd/pii/S026322411300300X>